ELSEVIER

Biophysical Chemistry 116 (2005) 67–76

Biophysical Chemistry

http://www.elsevier.com/locate/biophyschem

Glycolytic oscillations and waves in an open spatial reactor: Impact of feedback regulation of phosphofructokinase

Satenik Bagyan[a], Thomas Mair[a,*], Etiennette Dulos[b], Jacques Boissonade[b], Patrick De Kepper[b], Stefan C. Müller[a]

[a]*Otto-von-Guericke-University of Magdeburg, Institute of Experimental Physic, Group of Biophysics, Universitätsplatz 2, D-39106 Magdeburg, Germany*
[b]*Centre de Recherche Paul-Pascal, CNRS Bordeaux, Avenue Schweitzer, F-33600 Pessac, France*

Received 3 November 2004; received in revised form 22 February 2005; accepted 23 February 2005
Available online 21 March 2005

Abstract

An open spatial reactor has been designed for the investigation of spatio-temporal dynamics of glycolysis. The reactor consists of a diffusive layer made of gel-fixed yeast extract which is in contact with a continuously stirred reservoir to supply this layer with substrates. The coupling between reaction and diffusion in the gel layer enables the formation of spatio-temporal patterns.

Temporal oscillations of glycolysis are simply induced by feeding the yeast extract with sugar. Under properly chosen conditions, these oscillations sustain for more than 12 h. A necessary prerequisite for the generation of oscillations is that the ATP concentration in the feeding solution must be high enough to allow for negative feedback of phosphofructokinase. Otherwise, the interplay between ATP-consuming and ATP-producing reactions leads to an unfavorable low ATP/AMP ratio.

The generation of travelling NADH-waves is observed in the diffusive layer, when feeding the yeast extract with substrates. Break-up of circular-shaped waves is repeatedly observed, resulting in the formation of rotating NADH-spirals.

Keywords: Supply–demand; Energy charge; Ultrafiltration membrane; Spatio-temporal pattern formation; Reaction–diffusion coupling; Continuous stirred tank reactor

1. Introduction

Periodic behaviour is a fundamental property of living systems and is found at different levels of biological organization as for example, the circadian rhythm [1,2], the cell cycle [3,4], glycolytic oscillations in yeast cells [5,6] and extract [7], heart cells and extract [8,9], pancreatic β-cells [10] and muscle extract [11].

A characteristic feature of oscillatory systems is their ability to generate stationary or dynamic spatio-temporal patterns. The appearance of reaction–diffusion waves in different biological systems is well documented, e.g. such as calcium waves in frog oocytes [12], spreading depression waves in the cortex [13], and retina [14], cyclic AMP waves in cell layers of the slime mould *Dictyostelium discoideum* [15], NADH waves in neurophils [16] and in yeast extract [17,18] (for an extended review see [19]).

We investigate the mechanism of metabolic pattern formation in a yeast extract. For this we focus on oscillatory glycolytic degradation of sugar which plays a central role for the regulation of the energy metabolism of cells. A necessary prerequisite for a precise investigation of such a system in nonequilibrium is to have it operated in an open reactor. Several groups have studied the temporal dynamics of glycolysis in a continuous stirred tank reactor (CSTR)

Abbreviations: PFK, phosphofructokinase; ALD, aldolase; GAPDH, glyceraldehyde-3-phosphate dehydrogenase; PGK, phosphoglycerate kinase; PK, pyruvate kinase; G6P, glucose-6-phosphate; F6P, fructose-6-phosphate; FDP, fructose-1,6-diphosphate; GAP, glyceraldehyde-3-phosphate; DAP, dihydroxyacetone phosphate.

* Corresponding author. Tel.: +49 391 67 11681; fax: +49 391 67 11181.
E-mail address: thomas.mair@physik.uni-magdeburg.de (T. Mair).

0301-4622/$ - see front matter © 2005 Elsevier B.V. All rights reserved.
doi:10.1016/j.bpc.2005.02.002

with yeast cells [20], yeast extract [21,22], or purified glycolytic enzymes [23,24]. However, these studies did not take up the formation of spatial patterns.

The study of sustained spatio-temporal patterns is only possible in an open spatial reactor. Standard reactors of this sort consist of a diffusive layer in contact with the contents of a CSTR. The former, often a disc of hydrogel, prevents any hydrodynamic flow but allows both for reaction and for diffusion within the gel. Permanent nonequilibrium conditions are insured in the gel by diffusive exchanges of matter between the CSTR and the gel at the contact interface. Such open spatial reactors have been used to investigate travelling waves in the Belousov–Zhabotinsky reaction [25,26] or stationary patterns in the CIMA reaction [27–29]. We have adapted such a reactor for the investigation of spatial reaction–diffusion patterns in the glycolytic reaction by trapping a yeast extract in the gel part of the reactor and by feeding the CSTR with sugar and co-factors of the glycolytic reactions.

2. Materials and methods

2.1. Preparation of yeast extract

All experiments were performed with a cell-free yeast extract prepared from the aerobically grown yeast *Saccharomyces carlsbergensis* (ATCC 9080) according to ref. [30], except that the phosphate buffer was replaced by 25 mM MOPS pH 6.5, 50 mM KCl. The yeast cells were ruptured with glass beads (diameter: 0.45–0.5 mm) in a Braun–Melsungen homogenizer.

2.2. The open spatial reactor

The open spatial reactor is made of two parts: the lower part is a CSTR in which solutions of substrates and co-factors for glycolysis are permanently injected by means of a peristaltic pump (see Scheme 1) and are constantly mixed by a magnetic stirrer. The upper part consists of a disc of gel being indirectly in contact with the solution in the CSTR. A set of two circular membranes is placed between the gel and the CSTR: a black nitro-cellulose membrane with pore size of 0.8 μm from Millipore tightly placed on a cellulose triacetate membrane, MW cut off 10 kDa, from Sartorius.

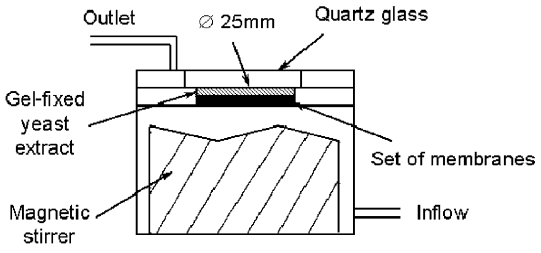

Scheme 1. Schematic drawing of the open spatial reactor. For explanation see text.

The black membrane strongly reduces the fluorescence background from the white Sartorius membrane and largely improves the detection of the NADH-fluorescence of the yeast extract.

The role of the membrane is not only to keep the enzymes within the gel but also to partly decouple the gel contents from the CSTR contents, in order to form spatial patterns. In the absence of this decoupling, the homogeneous (stirred) state of the CSTR would force the thin film of the gel to be also homogeneous.

2.3. Gel fixation of yeast extract

6.1% agarose (Type IXA from Sigma) in deionized water (conductivity ≤ 0.056 μS × cm) was heated for 5–7 min at 65 °C. The melted gel was placed in a water bath at 23 °C. At the same time 0.98 ml of yeast extract (30 mg protein/ml) was also incubated at 23 °C. After 2–3 min, the yeast extract was carefully mixed with the agarose (end concentration: 1.65%). This mixture was then placed between 2 glass plates separated by spacers 1.3 mm thick. A 5-kg weight was placed on the upper glass plate (20 cm × 15 cm) for 15 min in order to obtain a flat surface of the gel. During this gelation process the temperature was kept at 0 °C by ice containers. Thereafter, a circular piece (diameter: 24 mm) was cut out of the gel slide and placed on the black Millipore membrane. The volume of the circular piece of gel was 588 μl.

2.4. Experiment

Before the start of the experiments, each membrane (Sartorius and Millipore) was soaked in the deionized water for 2 h. As described above, the gel loaded with yeast extract was placed on the set of two membranes and then transferred into the reactor. The upper face of the gel was pressed against a quartz window. Time zero of experiments is when injection of feeding solutions in the CSTR starts.

The residence time in the reactor was 26 min. The following feeding solution was used (*end concentrations in the total input flow*): ATP—0.6 mM, ADP—0.4 mM, NAD—0.8 mM, MOPS—10 mM pH 6.5, $MgCl_2$—3 mM, Trehalose—50 mM, KH_2PO_4—50 mM pH 6.5, KCl—100 mM. Changes of this solution are indicated in the text. The temperature in the reservoir of the reactor was kept constant at 21 °C.

2.5. Optical set up

The spatio-temporal dynamics of glycolysis in the yeast extract was monitored using the optical set up shown in Fig. 1. White light from a Xenon lamp (Laser 2000) was passed through an UG-11 filter (broadband filter, centered around 340 nm). The resulting light beam was reflected via a dichroic mirror (LINOS) to the yeast extract. Fluorescence light of NADH in the gel (460 nm) passed through the

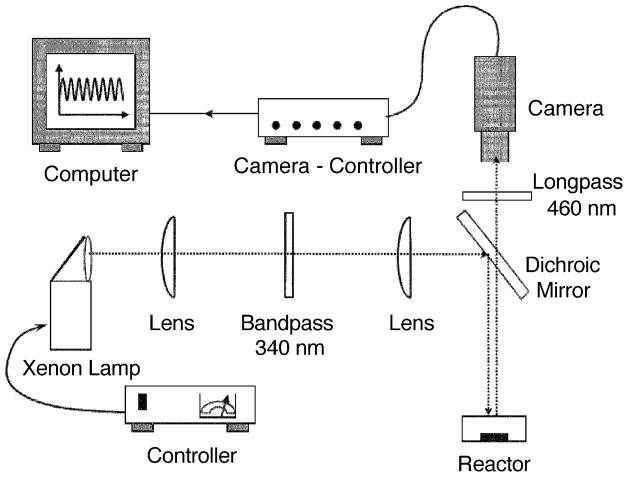

Fig. 1. Schematic drawing of the optical set up for monitoring spatio-temporal patterns of NADH. For experimental details see Materials and methods.

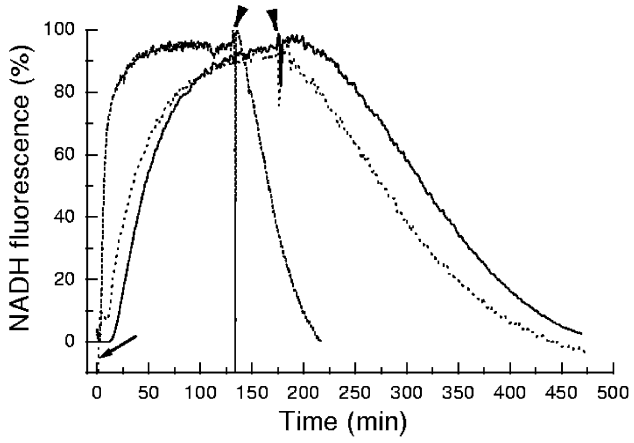

Fig. 2. Transport of NADH into the agarose gel (1.65%) through different types of membranes. Firstly, the reactor was fed with 50 mM KH_2PO_4 buffer, pH 6.5, which was replaced after 15 min ($t=0$ in the figure and indicated with arrow) by a solution of 1 mM NADH in 50 mM KH_2PO_4, pH 6.5. After 2 h the NADH solution was changed back to the buffer (arrow head). (—) Sartorius membrane, (- - -) Anodisc membrane, (• • • •) Schleicher & Schuell membrane. For each time trace the highest fluorescence value was taken as 100%.

dichroic mirror to an intensified camera, containing a bialkali–photocathode (Corail, Optronis-SG). In order to reduce noise from reflecting light, a 440-nm-long pass filter was placed directly in front of the camera objective. Digital movies were stored on a video tape (SONY video recorder EVT-801CE).

The temporal dynamics of the system was studied by following the local changes of the NADH fluorescence in the gel. For that, the grey levels of a selected small area (50×50 pixels $= 1.07$ mm $\times 1.07$ mm) were averaged and the arithmetic mean was then plotted as a function of time.

2.6. Measurement of glycolytic intermediates

Probes from the outlet of the reactor were collected at different phases of the glycolytic oscillations. The concentrations of glycolytic intermediates were measured in these probes by standard methods of enzymatic determination [31].

3. Results

3.1. Test of membrane permeability

Membranes play a crucial role in these experiments. Not only should they prevent flow of proteins out of the gel but also provide sufficient diffusion of substances from the reservoir of the reactor into the gel and back. In order to check the relevant diffusion properties of the membranes, we fed the reactor only with solutions of NADH in phosphate buffer. In this case the agarose gel was prepared only with water (no yeast extract). NADH is one of the main intermediates of glycolysis, its molecular weight being in the range of those of glycolytic intermediates, and it is easily monitored by its intrinsic fluorescence. The diffusion behaviour of NADH will therefore provide qualitative information about the exchange of glycolytic intermediates through the membrane. Fig. 2 shows the kinetics of the NADH fluorescence increase in the gel when the reactor is fed with NADH solutions. Removing NADH in the feeding solutions results in a decrease of fluorescence in the gel, demonstrating an efficient communication through the membrane. This experiment was performed with 3 different types of membranes: An Anodisc membrane (Type: Anodisc 25, from Whatman company) with pore size of 20 nm, a nitrocellulose membrane with MW cut off 10 kDa (Schleicher & Schuell), and a cellulose triacetate membrane with MW cut off 10 kDa from Sartorius company.

The initial velocities of the NADH fluorescence change obtained with these membranes are listed in Table 1 for comparison. The results show that the Anodisc membrane has by far the highest permeability. In control experiments, this membrane has been proven to support the formation of Turing patterns in the chemical CIMA reaction in this reactor. However, the Anodisc membrane is not appropriate

Table 1
Initial velocities of NADH transport through different types of membranes

Type of membrane	V_{in} (%/min)	V_{out} (%/min)
Sartorius membrane—10 kDa	1.6 ± 0.04	0.47 ± 0.01
Sartorius+black membrane	1.16 ± 0.2	0.8 ± 0.17
Schleicher & Schuell—10 kDa	1.38 ± 0.05	0.46 ± 0.007
Anodisc membrane	14.75	1.65

The data have been calculated from fluorescence measurements as shown in Figs. 2 and 4. They are expressed in % of NADH fluorescence change per minute. The maximal fluorescence change was taken as 100%. The mean of 3 different experiments together with the S.E.M. is shown, except for the Anodisc membrane, where only 1 representative experiment is given. The first column of the table shows the initial velocity of NADH diffusion into the gel (V_{in}); the second column shows the initial velocity of NADH disappearance out of the gel (V_{out}).

for our experiments because the pore size is too large (larger than the size of enzymes). Membranes from Sartorius or Schleicher & Schuell company have smaller pore sizes (10 kDa) and are designed for the retention of proteins. The data show that transports through the Sartorius membrane and through the Schleicher & Schuell membrane are similar (Fig. 2 and Table 1). However, both membranes exhibit an undesirable background fluorescence which is larger for the Schleicher & Schuell membrane than for the product from Sartorius. Therefore, we have chosen Sartorius membranes for our experiments.

3.2. Calibration of NADH fluorescence

Fig. 3 illustrates the calibration of the fluorescence intensity of NADH. For this purpose, discs of agarose gel containing different NADH concentrations were placed either directly on the Sartorius membrane or on a set consisting of the Sartorius membrane covered by a black membrane (see Materials and methods for details). These discs of gel were then placed into the reactor (without solutions) and fluorescence of NADH was measured with the optical set up shown in Fig. 1. As a control, NADH solutions in quartz cuvettes were also measured with this set up. When using only the Sartorius membrane as a support for the gel we found a saturation of the fluorescence signal for concentrations exceeding 0.5 mM NADH. We have measured the autofluorescence of the Sartorius membrane and found that it exhibits a high fluorescence at 460 nm when excited at 340 nm. This may explain why the NADH calibration curve comes into saturation when the Sartorius membrane is used. When monitoring NADH solution in a quartz cuvette (without membrane) we find a linear relationship between NADH fluorescence and concentration up to 1 mM. Covering the white Sartorius membrane with a black Millipore membrane (pore size 0.8 μm) eliminates the background fluorescence from the Sartorius membrane and yields similar results as with the cuvette (Fig. 3).

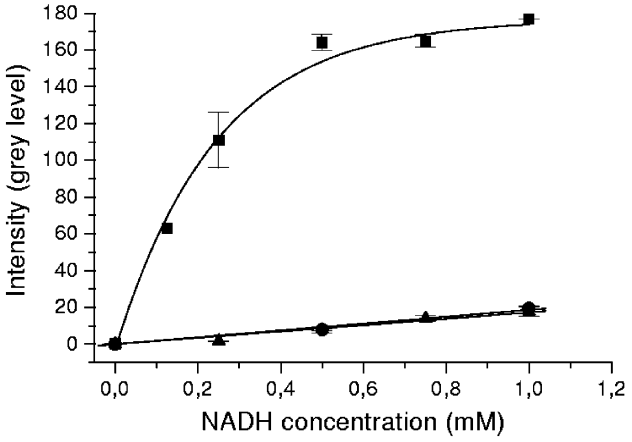

Fig. 3. Fluorescence intensity as a function of NADH concentration. For experimental procedure see text. NADH fluorescence was measured in an agarose gel placed on the Sartorius membrane (■), or on the set made of black and Sartorius membranes with the black membrane on top (●), or in a quartz cuvette (▲). The solid lines represent fits of the experimental data with either a linear fit (circles and triangles) or a first-order exponential decay function (squares).

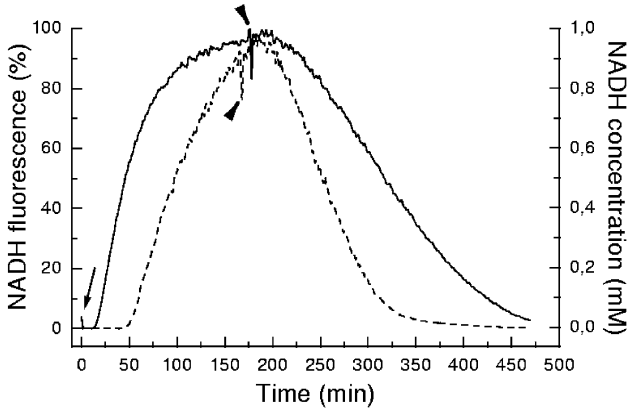

Fig. 4. Decrease of NADH transport velocity with the set of 2 membranes. The time trace for NADH transport through the set of the Sartorius and black membrane (- - -) and through the Sartorius membrane alone (—) is shown. The left ordinate shows normalized NADH fluorescence and the right ordinate the corresponding NADH concentration. The arrow indicates replacement of the phosphate buffer with 1 mM NADH solution and the arrow heads the return back to the buffer. Experimental procedure as described for Fig. 2.

The permeability of the set of membranes is different from that of the uncovered Sartorius membrane (Fig. 4 and Table 1). When this set was used, the initial velocities of NADH transport into the gel decreases by 28%, whereas the initial velocity of NADH transport out of the gel was increased by about 70%. This results in similar transport velocities through the membrane set in both directions.

3.3. Glycolytic oscillations and effect of adenine nucleotides

The permanent supply of fresh reactants in the open spatial reactor allows to maintain the system far away from equilibrium and in a constant and well-defined state with respect to a closed system. For inducing oscillatory glycolysis we need to feed the yeast extract with the substrate of glycolysis (sugar). Since there is also a permanent diffusion of substances out of the gel, it is required to feed all low molecular weight components, which are necessary to maintain oscillatory glycolysis, as for example, salts and buffer. In particular, adenine and pyridine nucleotides have to be fed because they are tightly connected to the glycolytic pathway but are not synthesized during glycolysis.

Glycolytic oscillations in the open spatial reactor under continuous feeding and stirring are displayed in Fig. 5. After an initial adaptation time (not shown), we find oscillations with a period of 5.5 min. Due to the openness of the reactor oscillations should last as long as the reactor is fed with substrates, however, they already damp out after about 2 h. There are several possible reasons for this damping. For example, 1) the pores of the membrane could be clogged, 2) there might be a leak of an unknown metabolite, 3) some

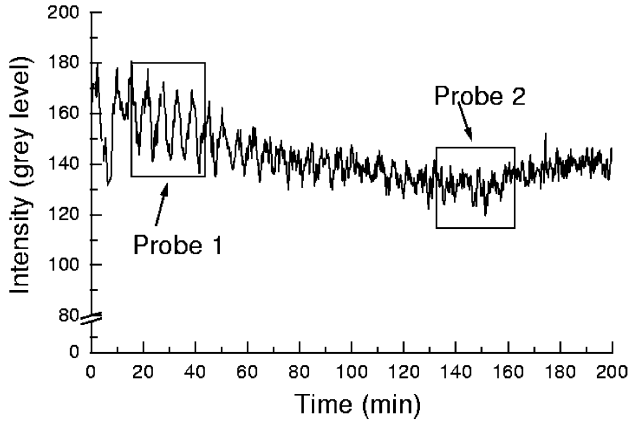

Fig. 5. Glycolytic oscillations of the yeast extract in the open spatial reactor. The reactor was continuously fed with trehalose, non-recycling substrates, salts and buffer (for recipe see Materials and methods). Stirring rate: 500 rpm, feeding rate: 6.6 ml/h. The rectangular boxes mark the time intervals during which probes from the outlet of the reactor were taken for the enzymatic analysis of glycolytic intermediates (cf. Fig. 6).

undetermined substances would additionally be required, 4) the enzymes might be destroyed, and 5) the ratio of the adenine nucleotides might be inappropriate to support oscillations. Generally, the problem could originate either in the composition of the feeding solution or in the yeast extract kinetics/components.

In order to check metabolic changes associated with this damping process, we have analysed the concentrations of various glycolytic intermediates from the outlet of the reactor. The results are shown in Fig. 6. The concentrations of all species vary from the oscillatory to the damped phase. Most pronounced are changes in the concentrations of adenine nucleotides: ATP decreases 33 times and AMP increases 7 times. These changes point out a strong activation of the enzyme phosphofructokinase (PFK) at the transition from the oscillatory to the damped phase. The decrease of the concentration of ATP, the inhibitor (and substrate) for this enzyme, and the concomitant increase of the concentration of the activator (AMP) results in a full opening of the PFK (no negative

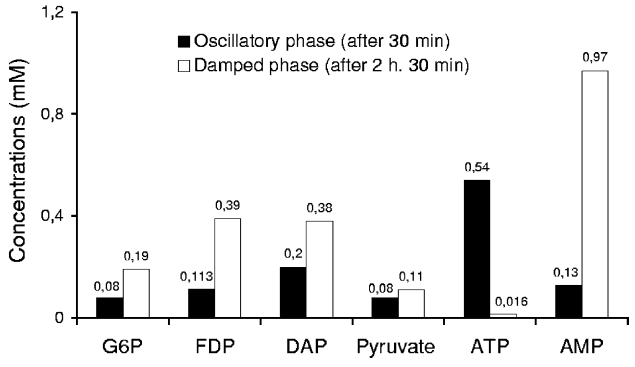

Fig. 6. Determination of glycolytic intermediates during the oscillatory and the damped phases. The probes were taken at the time instants marked in Fig. 5 as probes 1 (after 30 min) and 2 (after 2 h 30 min), respectively. For experimental procedure see Materials and methods.

feedback), which is also confirmed by the 3.5-fold increase in fructose-1,6-diphosphate (FDP) concentration in this experiment.

We suggest that the supply of ATP (by the pump) was smaller than the demand (activity of kinases), so that the adenylate kinase (AK) converts most ADP into ATP and AMP. Since ATP is further consumed we get a permanent production of AMP (see Scheme 2). To decrease the consumption of ATP by the PFK we added 4 mM FDP to the feeding solution. As a result there is no more a large increase of FDP in the eluate of the reactor (Fig. 7). However, we still find the strong decrease in ATP and concomitant increase in AMP, indicating that the supply–demand problem is still present. Therefore we tried to reduce also the consumption of ATP by hexokinase (HK) by adding the product of this enzyme, glucose-6-phosphate (G-6-P), to the feeding solution. Additionally, we increased the concentrations of adenine nucleotides (increased supply) and KH_2PO_4 (for reducing the ATPase activity) in the feeding solution. When running the reactor under these conditions, the analysis of the glycolytic intermediates in the eluate demonstrates that the ratio of the adenine nucleotides does not markedly change during the first 4 h of feeding, indicating that the

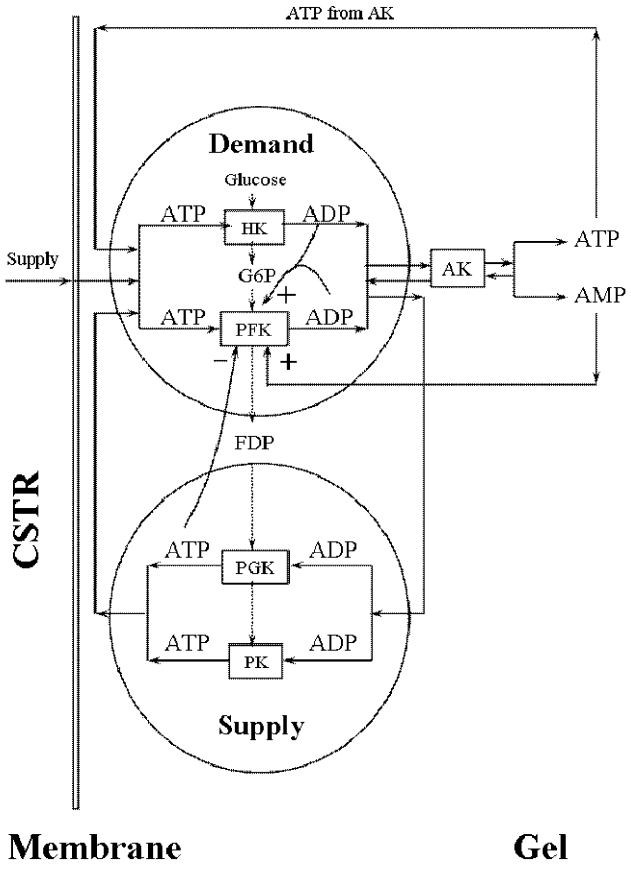

Scheme 2. Model for the control of glycolytic oscillations in the open spatial reactor, based on feedback regulation of the Phosphofructokinase. For explanation see text.

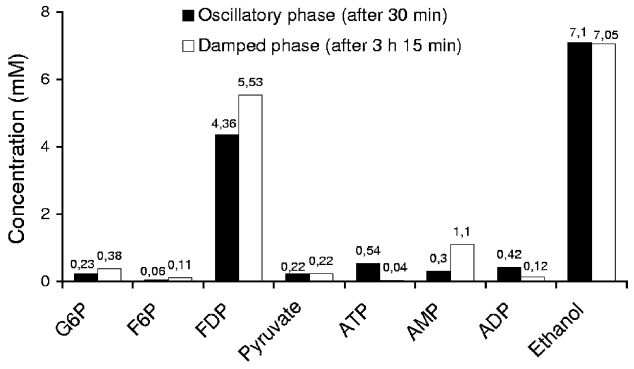

Fig. 7. Effect of fructose-1,6-diphosphate on the oscillatory transition. The yeast extract was fed with the same solutions as for Fig. 5, except that 4 mM FDP was additionally included. The probes were taken during the oscillatory phase (30 min after start of feeding) and after damping of the oscillations (3 h 15 min after start of feeding). Other experimental procedure as described in Materials and methods.

supply–demand problem is now solved (Fig. 8). This increases the duration of the oscillatory phase, which is now doubled. However, we still find damping, indicating that additional, yet unknown factors are required to support sustained oscillations. This can also be deduced from measurements with a different preparation of yeast extract. With this new preparation, we always get longer lasting oscillations (Fig. 9), indicating that the molecular composition of this extract is superior. In this case we have an oscillatory phase of 6 h when feeding with a recipe as described for the experiment shown in Fig. 6. Oscillations are prolonged for more than 12 h (Fig. 10) after increasing the metabolites concentration as described for Fig. 8. When feeding was stopped, we observed a transient increase and subsequent strong decrease of the NADH fluorescence, demonstrating that the communication between the feeding chamber and the gel is still working.

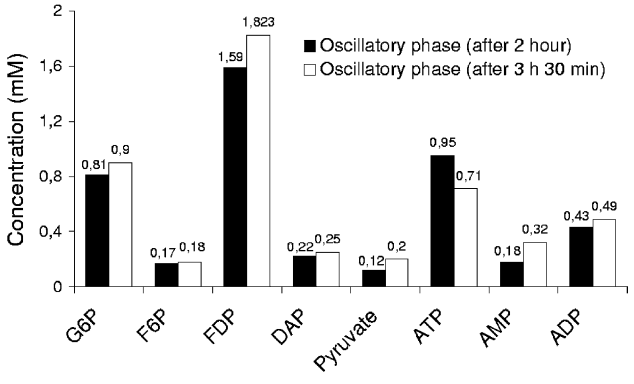

Fig. 8. Effect of increased supply of adenine nucleotides on the glycolytic oscillations. The feeding solution contained (final concentrations in the total input flow): ATP—0.84 mM, ADP—0.66 mM, FDP—1 mM, G-6-P—1 mM, $MgCl_2 \cdot 6H_2O$—3.5 mM, NAD—0.8 mM, KH_2PO_4—100 mM pH 6.5, KCl—100 mM, Trehalose—50 mM. Note, that the FDP concentration was reduced from 4 mM to 1 mM. For comparison with the results shown in Fig. 7, the probes were taken 30 min and 3 h 30 min after start of feeding (both in the oscillatory phase). For experimental details see Materials and methods.

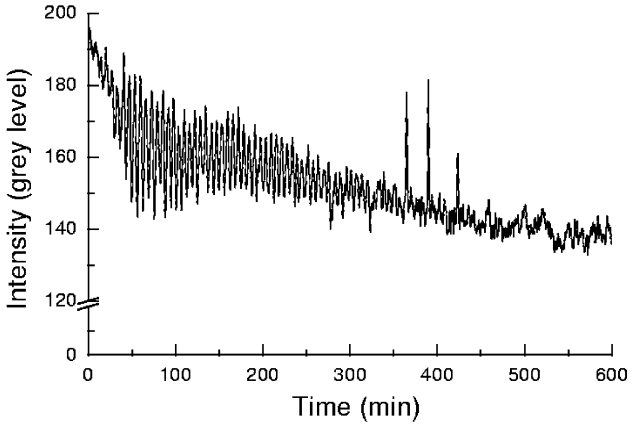

Fig. 9. Effect of preparation of yeast extract on duration of glycolytic oscillations. For this experiment a new preparation of yeast extract was used (preparation 5). All other experimental conditions were the same as described for Fig. 5.

3.4. Spatio-temporal patterns

When there is the coupling between an autocatalytic reaction and transport, oscillatory glycolysis is associated with the generation of reaction–diffusion waves. This has been shown by theoretical analysis [32] and later confirmed by experimental results [17,18]. The open spatial reactor has a diffusive layer (gel-fixed yeast extract) supporting the coupling of reaction and diffusion, which is a sufficient condition for the formation of spatio-temporal patterns. In fact we could frequently observe the formation of reaction–diffusion waves.

Fig. 11 displays the results of travelling NADH waves, as observed in the experiment shown in Fig. 10. After an initial time period of about 20 min, NADH waves were spontaneously generated. They propagate from the border of the gel to the center. The velocity of the waves has been calculated at different time points of the experiment (Fig. 12) using a time–space plot (an example of such a time–space plot is shown in Fig. 13). The velocity for each wave

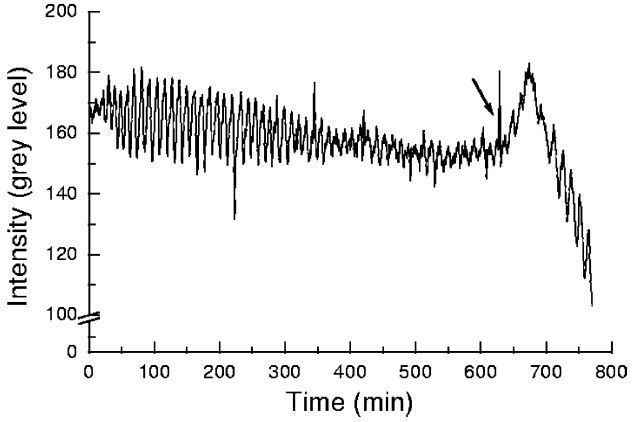

Fig. 10. Sustained glycolytic oscillations in the open spatial reactor. The experiment was performed with preparation 5. All other experimental conditions were as described for Fig. 8 (increased concentrations of ATP, ADP). Stop of feeding at 610 min is indicated by an arrow.

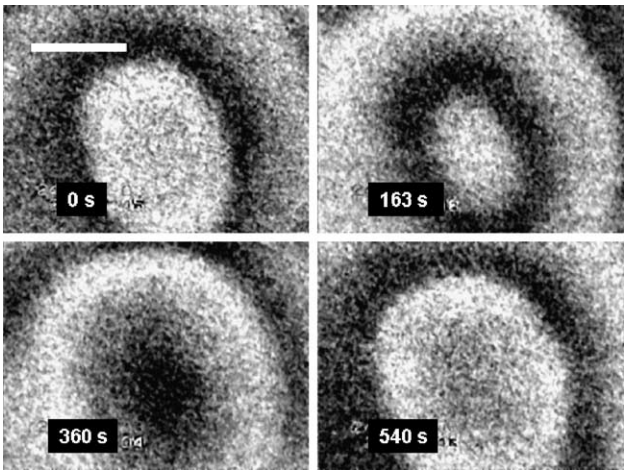

Fig. 11. Spontaneous generation of circular NADH waves in the open spatial reactor. The temporal behaviour of the yeast extract is shown in Fig. 10. The spatial distribution of NADH in the gel was monitored with a camera (see Materials and methods). After an induction time circular NADH waves propagate from the border of the gel to the centre. Time interval between successive images is indicated. Scale bar: 5 mm. Wavelength is about 6 mm, diameter of the waves is about 4.5 mm. The bright regions correspond to increased concentrations of NADH.

is constant, but for subsequent following waves there is a fast decrease of the velocity during the first 3 h until it approaches a constant value of about 7 μm/s. The kinetics of this decrease can be fitted with a first order exponential decay function, indicating that a diffusion equilibrium between the gel and CSTR takes place. The fact that after an initial adaptation time a constant velocity is observable for several hours demonstrates that a true open state can be achieved. For comparison with a closed system, the velocity of subsequent waves in a batch experiment is shown in Fig. 14 (for experimental procedure see [17]). Here, we find a decrease of the wave velocity for every subsequent wave. In the same way, after feeding was stopped, a decrease of the wave velocity in the open reactor from about 7 μm/s to 5

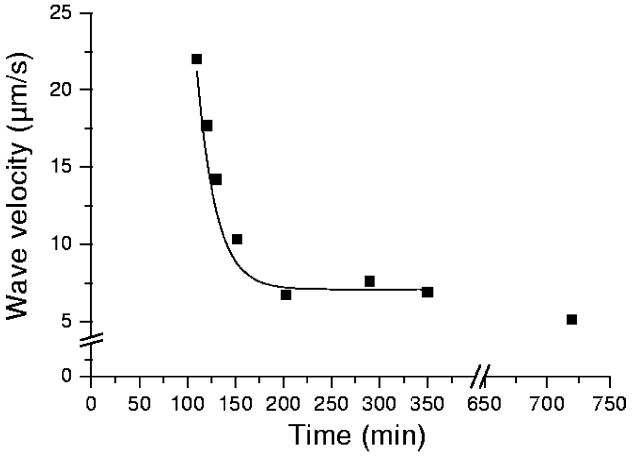

Fig. 12. Constant wave velocity after an initial adaptation time. The squares represent experimental data, the full line is a first-order exponential decay fit of these data. The decreased velocity at 720 min results from stop of feeding after 610 min.

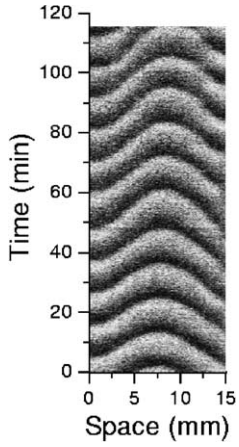

Fig. 13. Time–space plot of propagating NADH waves. The plot was constructed from a movie taken for the experiment shown in Fig. 10 as follows: the intensity profile along a horizontal line was plotted for all images between 173 min and 290 min as a function of space (*X*-axis) and time (*Y*-axis). The slope of the lines is a measure of the wave velocity.

μm/s (Fig. 12) was observed, indicating that the system is now no longer in an open state.

4. Discussion

We have designed an open spatial reactor for investigation of glycolytic reaction–diffusion waves in a layer of yeast extract under well-defined and constant conditions. In this reactor reaction–diffusion coupling is achieved by fixation of the yeast extract with agarose gel. Openness of the system is maintained by constant feeding of this gel with substrates. When feeding the yeast extract with sugar we can observe glycolytic oscillations for more than 12 h. There is an induction time, during which obviously an equilibration between the gel and the feeding solution takes place, because their metabolic/ionic composition is different. This

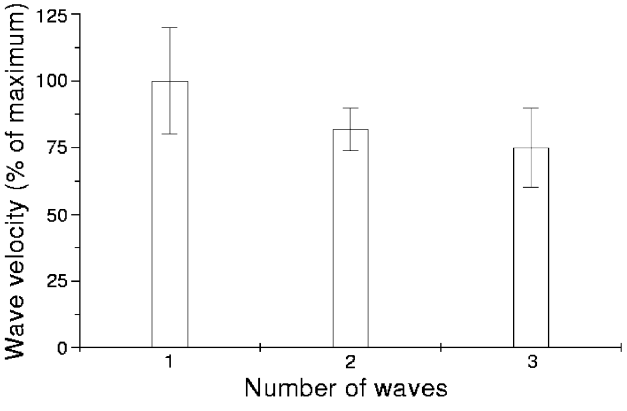

Fig. 14. Decrease of the velocity of subsequent following NADH waves in a yeast extract under batch conditions. Glycolytic waves (1–3) have been measured as described in [17]. The velocity is expressed as % of maximum, where the velocity of the first wave is taken as the maximum. The results represent the mean of 3 different experiments. The standard deviation of these results is shown as error bars.

adaptation process is reflected by the exponential decrease of the wave velocity (which becomes constant after 3 h) and the decrease of the NADH amplitude, which reaches a constant value after 2 h.

We used the disaccharide trehalose for feeding of the yeast extract. This sugar is split into 2 units of glucose by the enzyme trehalase. Since this enzyme works at low activity in the yeast extract (30 nmol/mg protein × min, [33]), there is a slow and constant input of glucose into glycolysis. This means, that the trehalose concentration can reach quite high concentrations throughout the gel and then can act as a "substrate buffer" for glycolysis. We assume that the rate of consumption of the trehalose (the input species into the gel) is small in regard to their total amount. This may explain, why oscillations with a period of about 5 min can be observed, although the typical diffusion time perpendicular through the gel is estimated to be 28 min for the 1.3 mm thick gel.

An important prerequisite for the maintenance of constant glycolytic oscillations is a proper balance between the ATP-consuming and ATP-providing processes as has been already reported for oscillatory glycolysis under batch conditions [34]. If this balance is perturbed, the glycolytic oscillations damp out (see Figs. 6 and 9). Our explanation for this damping is based on the feedback regulation of PFK by ATP (inhibitor) and ADP, AMP (activators) [35] (see Scheme 2).

When the ATP concentration in the feeding solution is too low, all ATP is consumed in the upper part of glycolysis by HK and PFK for phosphorylation of glucose. This occurs during the transition from the oscillatory to the damped state (see Figs. 6 and 7). As a result, feedback inhibition of PFK by ATP is no longer possible. On the other hand, the increasing concentration of ADP results in activation of the PFK. This increased kinase activity even enlarges the consumption of ATP, so that the demand for ATP for phosphorylation of glucose overcomes the supply of ATP. The exponential increase in ADP leads to a shift of the equilibrium of the AK to the formation of AMP and ATP. Due to the imbalance between supply and demand, the ATP produced from the AK reaction is immediately consumed by the kinases, which results in the accumulation of AMP (see Figs. 6 and 7 and Scheme 2).

Under these ATP-limiting conditions, the PFK is fully activated (high concentration of AMP), whereas a negative feedback is no longer possible (too low ATP concentration). Accordingly, the nonlinearity of the PFK reaction is prevented, abolishing the oscillations. This leads to an increased PFK-mediated flux as demonstrated by the rise of the FDP concentration in the non-oscillatory state (Figs. 6 and 7).

A substantial effect of the ATP/ADP ratio on the glycolytic flux has been also observed in living cells. Koebmann et al. [36] report that an increased expression of ATPase in *Escherichia coli* cells markedly decreases the ATP/ADP ratio, which leads to a marked increase of the glycolytic flux. Such a condition is similar with the situation of our system in the damped phase, where the ATP/ADP ratio is getting low (Figs. 6 and 7). Similarly, Kroukamp et al. [37] found an increase of the flux through glycolysis when the ATPase activity of yeast cells was increased by addition of uncouplers, resulting in a decrease of the ATP/ADP ratio.

The results of theoretical metabolic-control analysis, performed by Thomas and Fell [38] to study the role of the ATP demand for control of the glycolytic flux, showed that its control depends primarily on the activation of PFK by AMP and on ADP inhibition of ATPase. These results support our view that control of PFK diminishes rapidly as AMP concentration increases.

Larsson et al. [39] used permeablized yeast cells to study the control of the glycolytic flux. By this method they were able to adjust the concentrations of the adenine nucleotides as well as other glycolytic intermediates within the cells. They found that the ATP/AMP ratio strongly depends on the initial concentration of ATP and glucose. Similar to our findings, low initial ATP concentrations were completely converted to AMP, whereas at higher ATP levels the ATP consumption was reduced and the AMP production was negligible. This was accompanied by a complete suppression of FDP formation and accumulation of G-6-P and F-6-P at high ATP concentrations. Larsson et al. explained this behaviour by a control of the glycolytic pathway through feedback inhibition of PFK by ATP. At low ATP concentrations an increased demand/reduced supply for ATP decreases the glucose consumption.

Hess et al. [34] have measured the ratios ATP/AMP and ATP/ADP during glycolytic oscillations in a yeast extract. They found that for the oscillatory state the ATP/AMP ratio lies between 2.47 and 2.6 and the ATP/ADP ratio between 1.5 and 2.5. Our measured value for the ATP/ADP ratio in the oscillatory ranges is 1.1 and is similar to the data from Hess et al. However, our results for the ATP/AMP ratio in the oscillatory phase are higher by a factor of 2. After the transition from the oscillatory to the damped state both ratios strongly decrease, reaching ATP/ADP = 0.05 and ATP/AMP = 0.016, respectively. These ratios are far away from the oscillatory domain as reported by Hess et al.

Schellenberger et al. [40] used an open reconstituted enzyme system consisting of PFK (ATP-consuming) and pyruvate kinase (ATP-producing) as well as glucose-6-phosphate isomerase and AK. They found different stationary states for this system with respect to the concentrations of intermediates, depending on the activity of PFK and PK. A transition between ATP-producing and ATP-consuming stationary states could be explained by the allosteric properties of PFK. A self-stabilisation of the energy charge could be achieved by increasing the activity of the PK [41].

All these data demonstrate that the flow through glycolysis strongly depends on the ATP and AMP concentrations. To our opinion the mechanisms that realize this

control are located in the allosteric feedback control of PFK. A negative feedback is required in order to reduce the flow through this enzyme. This ensures that the activity of the kinase is small enough in order to maintain a "reasonable" energy charge. If the ATP concentration falls below a critical value, the missing negative feedback as well as the strong positive feedback by AK-generated AMP leads to a full opening of the PFK. This in turn leads to a nearly complete break down of ATP, such that ATP becomes limiting for phosphorylation of glucose, i.e. the ATP-demand overcomes the ATP-supply. Our results also demonstrate, that oscillations of the glycolytic pathway can only occur, when the ATP concentration is large enough to permit negative feedback of PFK.

Other groups have obtained similar experimental results but based on theoretical analysis, came to different interpretations [42–45]. Calculation of the control coefficients yielded a strong control of glucose transport and ATPase activity over the glycolytic pathway, whereas PFK was nearly ineffective. To our opinion, this interpretation is not complete. Since both, glucose transport and ATPase activity, lead to a marked decrease of ATP, the allosteric properties of PFK cannot be neglected for control of glycolysis.

The transition from the oscillatory to the damped state in the open spatial reactor (see Fig. 5) is associated with a loss of negative feedback of PFK (see Figs. 6 and 7). We tried to restore this negative feedback by increasing the ATP concentration in the feeding solution, as well as by reducing the kinase activities by increasing the supply of products (glucose-6-phosphate and fructose-1,6-diphosphate). In fact, this intervention did lead to the predicted prolongation of the glycolytic oscillations (Fig. 10). This is also verified by the fact that the energy charge remains nearly constant under these conditions (cf. Fig. 8). This result also points out the importance of negative feedback regulation of PFK for the generation of glycolytic oscillations. Moreover, it demonstrates that the open spatial reactor is a powerful tool for the external control of biochemical systems.

A characteristic property of oscillatory systems is the formation of spatio-temporal patterns due to the coupling of an autocatalytic reaction with diffusion. The gel-fixed yeast extract represents a diffusive layer that enables reaction–diffusion coupling. Accordingly, we find the generation of travelling NADH-waves in this gel, associated with the appearance of glycolytic oscillations. These waves initially start to propagate from the border of the gel to the middle where they exhibit mutual annihilation (Fig. 11). Since there are no-flux-boundary conditions in the x–y plane of the gel, we suggest that the formations of local gradients at this site are the causes for generation of the waves. The waves appeared about 20 min after the feeding of yeast extract with substrates was started and exhibited an exponential decrease of the wave velocity during the next 2 h. Break up of the waves and subsequent formation of rotating spirals can be repeatedly observed (Fig. 15). Presumably, local perturbations in the diffusion of substrates/products induce the break up of the waves. The mechanism of wave initiation and propagation is not yet clear: whether the waves represent phase waves or reaction–diffusion waves remains to be clarified in future studies.

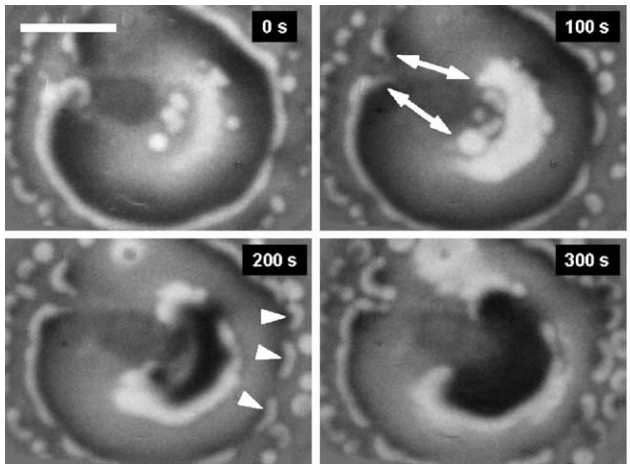

Fig. 15. Formation of rotating NADH-spirals. In this experiment the circular waves are generated in the center of the gel and are moved to the borders. Thirty minutes after start of the experiment these waves break up and form rotating double armed spirals (see arrows in image 100 s). Concomitantly, the wave back becomes destabilized and splits into small wave fragments (see arrow heads in image 200 s). Time interval between successive images is indicated. Scale bar: 5 mm. The bright regions correspond to increased concentrations of NADH.

Acknowledgements

We thank C. Warnke for help with the optical set up. U. Storb and R. Straube are acknowledged for help with computer programming. This work was financially supported by the Deutsche Forschungsgemeinschaft (DFG, SFB-555).

References

[1] E. Bünning, The Physiological Clock–Circadian Rhythms in Biological Chronometry, Springer Verlag, New York, 1973.
[2] F.W. Turek, Circadian rhythms, Horm. Res. 49 (1998) 109–113.
[3] C. Norbury, P. Nurse, Cyclins and cell cycle control, Curr. Biol. 1 (1991) 23–24.
[4] J.J. Tyson, B. Novak, Regulation of the eukaryotic cell cycle: molecular antagonism, hysteresis, and irreversible transitions, J. Theor. Biol. 210 (2001) 249–263.
[5] A. Ghosh, B. Chance, Oscillations of glycolytic intermediates in yeast cells, Biochem. Biophys. Res. Commun. 16 (1964) 174–181.
[6] P. Richard, B. Teusink, H.V. Westerhoff, K. van Dam, Around the growth phase transition *S. cerevisiae*'s make-up favours sustained oscillations of intracellular metabolites, FEBS Lett. 318 (1993) 80–82.
[7] B. Chance, B. Hess, A. Betz, DPNH oscillations in a cell-free extract of *S. carlsbergensis*, Biochem. Biophys. Res. Commun. 16 (1964) 182–187.
[8] R. Frenkel, Reduced diphosphopyridine nucleotide oscillations in cell-free extracts from beef-heart, Arch. Biochem. Biophys. 115 (1966) 112–121.

[9] B. O'Rourke, B.M. Ramza, D.N. Romashko, E. Marban, Metabolic oscillations in heart cells, Adv. Exp. Med. Biol. 382 (1995) 165–174.
[10] B.E. Corkey, K. Tornheim, J.T. Deeney, M.C. Glennon, J.C. Parker, F.M. Matschinsky, N.B. Ruderman, M. Prentki, Linked oscillations of free Ca^{2+} and the ATP/ADP ratio in permeabilized RINm5F insulinoma cells supplemented with a glycolyzing cell-free muscle extract, J. Biol. Chem. 263 (1988) 4254–4258.
[11] K. Tornheim, J.M. Lowenstein, The purine nucleotide cycle: III. Oscillations in metabolite concentrations during the operation of the cycle in muscle extracts, J. Biol. Chem. 248 (1973) 2670–2677.
[12] J. Lechleiter, S. Girard, E. Peralta, D. Clapham, Spiral calcium wave propagation and annihilation in *Xenopus laevis* oocytes, Science 252 (1991) 123–126.
[13] T.A. Basarsky, S.N. Duffy, R.D. Andrew, B.A. MacVicar, Imaging spreading depression and associated intracellular calcium waves in brain slices, J. Neurosci. 18 (1998) 7189–7199.
[14] M.A. Dahlem, S.C. Müller, Self-induced splitting of spiral-shaped spreading depression waves in chicken retina, Exp. Brain Res. 115 (1997) 319–324.
[15] K.J. Tomchik, P.N. Devreotes, Adenosine 3′,5′-monophosphate waves in *Dictyostelium discoideum*: a demonstration by isotope dilution–fluorography, Science 212 (1981) 443–446.
[16] H.R. Petty, R.G. Worth, A.L. Kindzelskii, Imaging sustained dissipative patterns in the metabolism of individual living cells, Phys. Rev. Lett. 84 (2000) 2754–2757.
[17] T. Mair, S.C. Müller, Travelling NADH and proton waves during oscillatory glycolysis in vitro, J. Biol. Chem. 271 (1996) 627–630.
[18] T. Shinjyo, Y. Nakagawa, T. Ueda, Hierarchic spatio-temporal dynamics in glycolysis, Physica, D 84 (1995) 212–219.
[19] B. Hess, Periodic patterns in biochemical reactions, Q. Rev. Biophys. 30 (1997) 121–176.
[20] S. Danø, P.G. Sørensen, F. Hynne, Sustained oscillations in living cells, Nature 402 (1999) 320–322.
[21] K. Nielsen, P.G. Sørensen, F. Hynne, H.-G. Busse, Sustained oscillations in glycolysis: an experimental and theoretical study of chaotic and complex periodic behavior and of quenching of simple oscillations, Biophys. Chem. 72 (1998) 49–62.
[22] C.G. Hocher, I.R. Epstein, K. Kustin, K. Tornheim, Glycolytic pH oscillations in a flow reactor, Biophys. Chem. 51 (1994) 21–35.
[23] W. Schellenberger, K. Eschrich, E. Hofmann, Self-organization of a glycolytic reconstituted enzyme system: alternate stable stationary states, hysteretic transition and stabilization of the energy charge, Adv. Enzyme Regul. 19 (1980) 257–284.
[24] J.-F. Hervagault, D. Thomas, Experimental evidence and theoretical discussion for long-term oscillations of phosphofructokinase in a compartmentalized system, Eur. J. Biochem. 131 (1983) 183–187.
[25] W.Y. Tam, W. Horsthemke, Z. Noszticzius, H.L. Swinney, Sustained spiral waves in a continuously fed unstirred chemical reactor, J. Chem. Phys. 88 (1988) 3395–3396.
[26] E. Dulos, J. Boissonade, P. De Kepper, Excyclon dynamics, in: A.V. Holden, M. Markus, H.G. Othmer (Eds.), Nonlinear Wave Processes in Excitable Media, Plenum, New York, 1991, pp. 423–434.
[27] V. Castets, E. Dulos, J. Boissonade, P. De Kepper, Experimental evidence of a sustained standing Turing-Type nonequilibrium chemical patterns, Phys. Rev. Lett. 64 (1990) 2953–2956.
[28] Q. Ouyang, H.L. Swinney, Transition from a uniform state to hexagonal and striped Turing patterns, Nature 352 (1991) 610–612.
[29] B. Rudovics, E. Barillot, P.W. Davies, E. Dulos, J. Boissonade, P. De Kepper, Experimental studies and quantitative modeling of Turing patterns in the (chlorine dioxide, iodine, malonic acid) reaction, J. Phys. Chem. (1999) 1790–1800.
[30] B. Hess, A. Boiteux, Mechanism of glycolytic oscillation in yeast: 1. Aerobic and anaerobic growth conditions for obtaining glycolytic oscillations, Hoppe–Seyler Z. Physiol. Chem. 349 (1968) 1567–1574.
[31] H.U. Bergmeyer, Methods of Enzymatic Analysis, vol. III, Verlag Chemie Weinheim/Academic Press Inc., New York, 1974.
[32] A. Goldbeter, Patterns of spatiotemporal organization in an allosteric enzyme model, Proc. Natl. Acad. Sci. 70 (1973) 3255–3259.
[33] B. Hess, K. Brand, Continuous oscillations in a cell-free extract of *S. carlsbergensis*, Biochem. Biophys. Res. Commun. 23 (1966) 102–108.
[34] B. Hess, A. Boiteux, J. Krüger, Cooperation of glycolytic enzymes, Adv. Enzyme Regul. 7 (1968) 149–165.
[35] E. Hofmann, K. Eschrich, W. Schellenberger, Temporal organization of the phosphofructokinase/fructode-1,6-bisphosphatase cycle, Adv. Enzyme Regul. 23 (1985) 331–362.
[36] B.J. Koebmann, H.V. Westerhoff, J.L. Snoep, D. Nilsson, P.R. Jensen, The glycolytic flux in *Escherichia coli* is controlled by the demand for ATP, J. Bacteriol. 184 (2002) 3909–3916.
[37] O. Kroukamp, J.M. Rohwer, J.-H.S. Hofmeyr, J.L. Snoep, Experimental supply–demand analysis of anaerobic yeast energy metabolism, Mol. Biol. Rep. 29 (2002) 203–209.
[38] S. Thomas, D. Fell, A control analysis exploration of the role of ATP utilisation in glycolytic–flux control and glycolytic–metabolite–concentration regulation, Eur. J. Biochem. 258 (1998) 956–967.
[39] C. Larsson, I.-I. Påhlman, L. Gustafsson, The importance of ATP as a regulator of glycolytic flux in *Saccharomyces cerevisiae*, Yeast 16 (2000) 797–809.
[40] K. Eschrich, W. Schellenberger, E. Hofmann, Transition between alternate ATP-producing and ATP-consuming stationary states in a reconstituted enzyme system containing phosphofructokinase, Acta Biol. Med. Ger. 41 (1982) 415–424.
[41] W. Schellenberger, K. Eschrich, E. Hofmann, Self-stabilization of the energy charge in a reconstituted enzyme system containing phosphofructokinase, Eur. J. Biochem. 118 (1981) 309–314.
[42] B. Teusink, B.M. Bakker, H.V. Westerhoff, Control of frequency and amplitudes is shared by all enzymes in three models for yeast glycolytic oscillations, Biochim. Biophys. Acta 1275 (1996) 204–212.
[43] K.A. Reijenga, J.L. Snoep, J.A. Diderich, H.W. van Verseveld, H.V. Westerhoff, B. Teusink, Control of glycolytic dynamics by hexose transport in *Saccharomyces cerevisiae*, Biophys. J. 80 (2001) 626–634.
[44] B. Teusink, J. Passarge, C.A. Reijenga, E. Esgalhado, C.C. van der Weijden, M. Schepper, M.C. Walsh, B.M. Bakker, K. van Dam, H.V. Westerhoff, J.L. Snoep, Can yeast glycolysis be understood in terms of in vitro kinetics of the constituent enzymes? Testing biochemistry, Eur. J. Biochem. 267 (2000) 5313–5329.
[45] M.A. Aon, S. Cortassa, H.V. Westerhoff, J.A. Berden, E. van Spronsen, K. van Dam, Dynamical regulation of yeast glycolytic oscillations by mitochondrial functions, J. Cell. Sci. 99 (1991) 325–334.